Paper:
Jones, M., Santín, C., van der Werf, G. & Doerr, S. (2019). Global fire emissions buffered by the production of pyrogenic carbon. *Nature Geoscience*
http://dx.doi.org/10.1038/s41561-019-0403-x

Submitted manuscript draft of version of: Jones, M.W., Santín, C., van der Werf, G.R., **Doerr, S.H.** (2019) Global fire emissions buffered by the production of recalcitrant pyrogenic carbon. *Nature Geoscience* (published on 5th Aug. 2019, available at: https://doi.org/10.1038/s41561-019-0403-x). Note that the published version will be an updated version from this submitted draft.

Global fire emissions buffered by the production of recalcitrant pyrogenic carbon

Authors:

Matthew W. Jones[1*], Cristina Santín[1,2], Guido R. van der Werf[3] and Stefan H. Doerr[1]

Affiliations:

[1]Geography Department, College of Science, Swansea University, Swansea, UK

[2]Biosciences Department, College of Science, Swansea University, Swansea, UK

[3]Faculty of Science, Vrije Universiteit, Amsterdam, Netherlands

*e-mail: matthew.w.jones@swansea.ac.uk.

Landscape fires burn an estimated 3-5 million km^2 of the Earth's surface annually, emitting 2.2 Pg C year^{-1} to the atmosphere while also converting a significant fraction of the carbon in burnt biomass to pyrogenic carbon (PyC) contained in combustion by-products. PyC can be stored in terrestrial and marine pools for centuries to millennia, buffering short-term emissions of carbon to the atmosphere by persisting as a recalcitrant pool of carbon during and following vegetation recovery. PyC stocks are routinely ignored in global models of the carbon cycle, leading to systematic errors in carbon accounting. Here we present a comprehensive new dataset of PyC production factors and merge this with the Global Fire Emissions Database (GFED4s+PyC) to quantify the global PyC production flux. GFED4s+PyC suggests that 256 (196-340) Tg C year^{-1} was converted to PyC by biomass burning in the period 1997-2016, 91% of which occurred in the (sub)tropics. While savannah fires were consistently the largest source of PyC (49% on average), variation in tropical forest burning, driven by the El Niño Southern Oscillation, was the dominant driver of inter-annual variability in global PyC production. Our global estimate equates to 12% of the carbon emitted annually by landscape fires, indicating that the fate of a substantial fraction of the vegetation carbon stocks affected annually by fire is misrepresented in fire-enabled global models. We estimate that the cumulative production of PyC since 1750 (60 Pg C) is equivalent to ~33-40% of the global losses of biomass carbon due to land use change in the same period. Our results show that PyC production creates capacity for a quantitatively significant sink for atmospheric CO_2 that is presently missing from global carbon budget assessments.

Globally, landscape fires including wildfires, deforestation fires, and agricultural burns emit approximately 2.2 Pg C year^{-1} to the atmosphere (1997-2016)[1]. This emission flux includes ~0.4 Pg C year^{-1} due to tropical deforestation and peatland fires, which contribute to net global emissions of carbon due to land use change (~1.1-1.5 Pg C year^{-1}; Figure 1)[2–4]. The emission fluxes resulting from biomass fires and land use change are outweighed by the re-sequestration flux of carbon to undisturbed and re-growing vegetation (~5.0 Pg C year^{-1}; Figure 1)[5–8]. These global carbon budget estimates are generated by models that represent the temporally distinct processes of immediate carbon emission from burned areas and decadal-scale re-sequestration through vegetation (re-)growth in a spatially explicit manner[1,9,10]. However, such models routinely overlook the coincident flux of biomass carbon to recalcitrant by-products of fire, which can be stored in terrestrial and marine pools for centuries to millennia, and thus provide a long-term buffer against fire emissions (Figure 1)[7,11–14]. Consequently, the legacy effects of fire that operate on the longest timescales are systematically excluded from models of the carbon cycle and from global carbon budgets[13,15].

These legacy effects are due to the incomplete combustion of vegetation during landscape fires, which transforms organic carbon (OC) in biomass to a continuum of thermally-altered products that are collectively termed pyrogenic carbon (PyC)[11,13,16]. The majority of the PyC produced during vegetation fires remains initially on the ground in charcoal particles of varying size and is subsequently transferred to its major global stores in soils[17–19], sediments[20,21] and ocean waters[22,23]. A smaller fraction of fire-affected vegetation carbon is emitted as PyC in smoke and has been studied extensively for its influence on Earth's atmospheric and cryospheric radiative balances[24,25]. PyC includes labile products of depolymerisation reactions as well as aromatic molecules that result from condensation reactions, the latter of which are depleted in functional groups and thus chemically and biologically recalcitrant[26–28]. The enhanced resistance of PyC to biotic and abiotic decomposition leads to its preferential storage in terrestrial and marine pools[16,21] and a residence time that is typically one to three orders of magnitude greater than that of its unburnt precursors[13]. This makes PyC one of the largest groups of chemically discernible compounds in soil with a contribution to soil organic carbon (SOC) stocks of 14% globally[17]. PyC is also conserved across the land-to-ocean aquatic continuum and thus contributes approximately 10% of riverine dissolved organic carbon[29], 16% of riverine particulate organic carbon[30], and 20-50% of the organic carbon in ocean sediments[14].

Submitted manuscript draft of version of: Jones, M.W., Santín, C., van der Werf, G.R., **Doerr, S.H.** (2019) Global fire emissions buffered by the production of recalcitrant pyrogenic carbon. *Nature Geoscience* (published on 5th Aug. 2019, available at: https://doi.org/10.1038/s41561-019-0403-x). Note that the published version will be an updated version from this submitted draft.

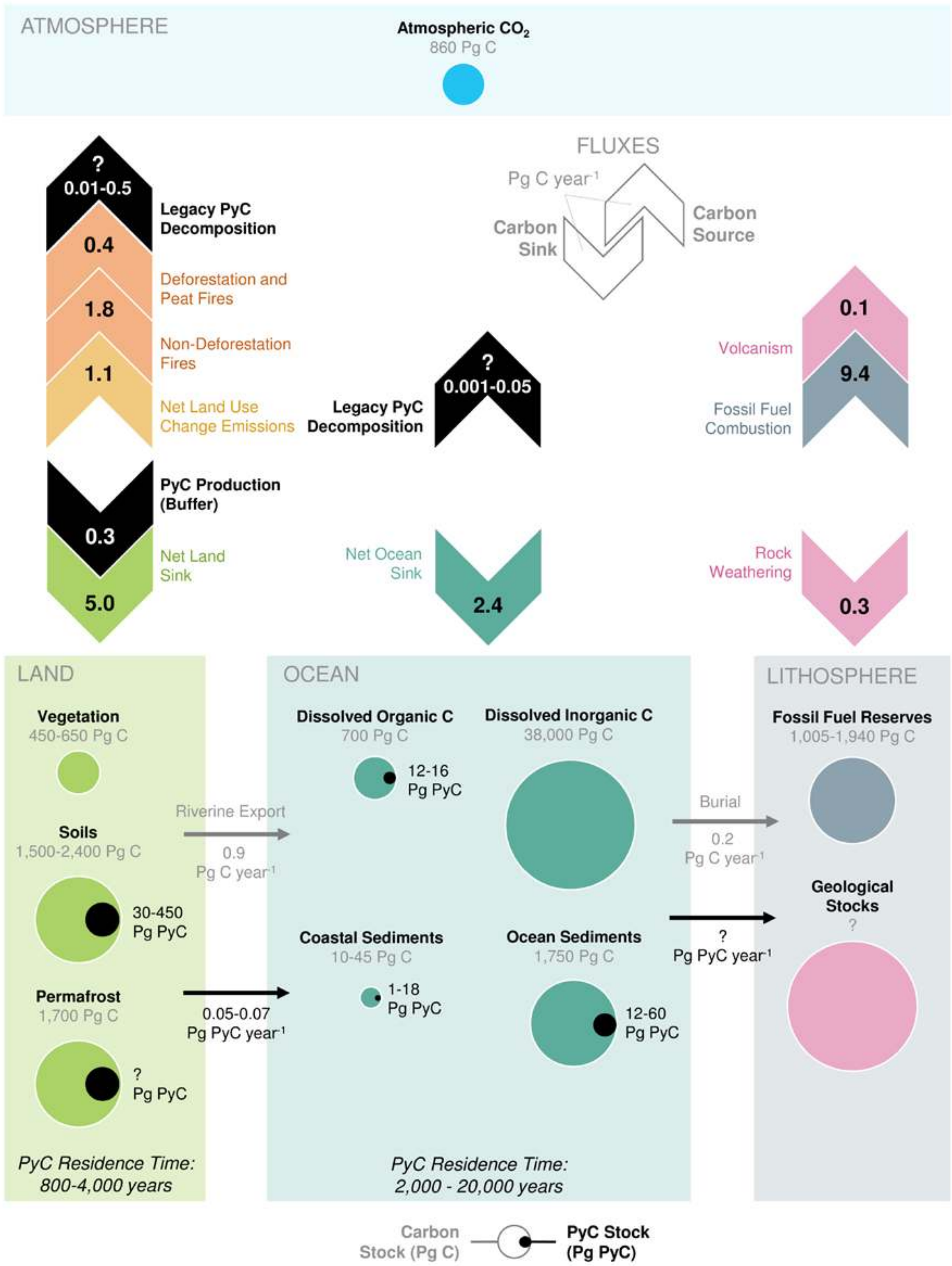

Figure 1: A simplified schematic of the global carbon cycle including the buffer and legacy roles of PyC. Stock values are expressed in Pg C (1 Pg C = 1 × 10^{15} g of carbon) and flux values are expressed in Pg C $year^{-1}$. The global carbon cycle is represented by values from the Global Carbon Budget assessment of the decade 2008–2017 (ref. [2]) including: stocks of carbon in vegetation, soil, permafrost, ocean dissolved organic and inorganic matter, coastal and oceanic sediments, and fossil fuel reserves; fluxes of carbon due to the net land sink

(modified to exclude non-deforestation fire emissions), fossil fuel combustion, the net ocean sink, and net land use change emissions (modified to exclude deforestation fire emissions). Emission estimates from deforestation and peat fires, and from non-deforestation fires derive from GFED4s and relate to the period 1997-2016 (ref. [1]; deforestation fires are restricted to the tropics). Carbon fluxes due to volcanism and rock weathering derive from the IPCC AR5 assessment and relate to the period 2000-2009 (ref. [4]). Pyrogenic carbon production fluxes due to deforestation and non-deforestation fires are based on estimates from GFED4s+PyC and relate to the period 1997-2016 (this study). PyC stocks in soils, oceanic DOC and ocean sediments are based on representative PyC/OC ratios from references [17], [31], and [14] applied to the Global Carbon Budget 2018 estimates of OC stocks and fluxes. PyC fluxes through rivers are the sum of global dissolved and particulate PyC export fluxes from references [29] and [30]. Residence times shown for soils derive from references [32] and [26]. Residence times for oceanic PyC pools derive from references [20] and [33]. Maximum (and minimum) legacy PyC decomposition fluxes for land and ocean stocks are calculated as the product of high-end (and low-end) total stock magnitudes in each domain and the reciprocal of the low-end (and high-end) estimate for residence time.

A series of reviews and data syntheses have recognised the potential of PyC production to invoke a drawdown (sink) of photosynthetically-sequestered CO_2 to pools that are stable on timescales relevant to anthropogenic climate change and its mitigation[7,11,13,14,34–37]. Owing to the relative recalcitrance of PyC, the conversion of biomass carbon to PyC represents an extraction of carbon from a pool cycling on decadal timescales to a pool cycling on centennial or millennial timescales[14,20,21,26,38]. This storage potential contrasts with that of dead vegetation, which otherwise contributes to post-fire emissions on annual to decadal timescales or enters soil pools with a shorter residence time than that of PyC[9,12,26,39,40]. Consequently, post-fire PyC pools emit carbon to the atmosphere over a significantly longer time period than would be the case in the absence of PyC production, meanwhile providing a buffer that moderates atmospheric CO_2 stocks (Figure 1)[7,13,14]. At present, the fire-enabled vegetation models that are used to make global carbon budget calculations account for short-term fire emissions but routinely exclude fluxes of carbon from biomass to PyC or the delayed emission of carbon from legacy PyC stocks to the atmosphere (Figure 1)[9,10,15,41,42]. This introduces systematic errors to global carbon budgets through misrepresentation of modern and historical fire effects on the net exchange of carbon between the atmospheric and terrestrial-marine pools[13–15].

While PyC has been recognised as a major component of post-fire carbon stocks for a number of decades[11,37], quantification of its production rate at the global scale has been problematic and estimates vary by roughly an order of magnitude (50-379 Tg C year^{-1})[13,14,36].

A cause of the large range of production estimates is that calculations have previously relied on incomplete information regarding the spatial distribution and type of fires, the allocation of carbon amongst biomass fuel components in burned areas and the specific PyC production factors for these distinct biomass fuel components. To alleviate these issues, we enhanced the Global Fire Emissions Database version 4 with small fires (GFED4s)[1], which is one of the principal process-based models used to make estimates of carbon emission from open biomass burning[41,43,44]. Specifically, PyC production was incorporated by following a three-step approach consisting of: *(i)* the assembly of the most comprehensive global database of PyC production factors (P_{PyC}; g PyC g^{-1} C emitted) compiled to date; *(ii)* the assignment of production factors for individual fuel classes stratified as coarse or fine and as woody or non-woody (Figure 2), and; *(iii)* the application of production factor (P_{PyC}) values to fuel-stratified carbon emissions (CE; g C emitted) modelled by the native fuel consumption model in GFED4s. The output is the first global gridded dataset for monthly PyC production at a resolution of 0.25° × 0.25°, covering the years 1997-2016.

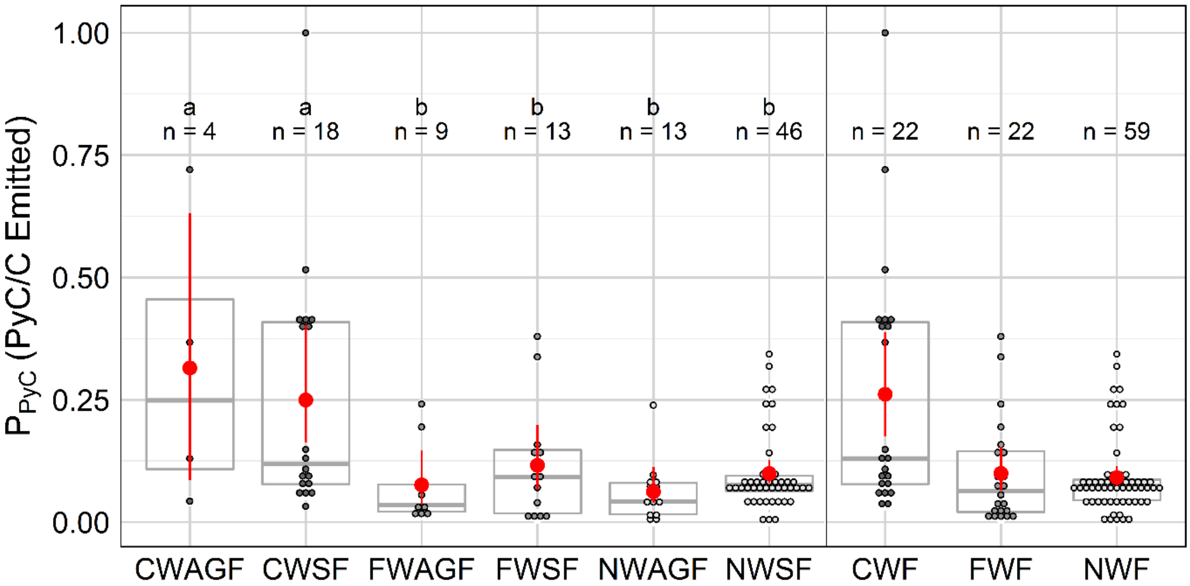

Figure 1: Box plots showing the distributions of PyC production factor (P_{PYC}) values for each of the biomass component classes in the production factor dataset. Abbreviations are: CWAGF, coarse woody aboveground fuels; CWSF, coarse woody surface fuels; FWAGF, fine woody aboveground fuels; FWSF, fine woody surface fuels; NWAGF, non-woody aboveground fuels; NWSF, non-woody surface fuels; CWF, coarse woody fuels (includes both CWSF and CWAGF); FWF, fine woody fuels (includes both FWAGF and FWSF); NWF, non-woody fuels (includes both NWAGF and NWSF). Dots mark the distribution of P_{PyC} values across 1% intervals

on the y-axis. Red dots show mean P_{PyC} values while red lines show the bootstrapped 95% confidence interval (see methods). Boxes illustrate the median and interquartile range of values. Letters a and b indicate biomass components with statistically similar P_{PYC} distributions at the 95% confidence level according to Tukey HSD tests. The number of data entries (n) is also shown.

Global PyC Production

Our central estimate for global PyC production in the period 1997-2016 was 256 Tg C year^{-1} with an uncertainty range based on production factors of 196-340 Tg C year^{-1} (Figure 3). Inter-annual variability in global PyC production, expressed as the standard deviation around the mean, was 47 Tg C year^{-1} and was most strongly associated with variability in woody fuel combustion, including standing wood and coarse woody debris (CWD; supplementary information text S1 and Figure S1). Coarse woody fuels produce PyC at a greater rate than finer fuels (Figure 2) and consequently forest fires have disproportionate potential to influence global rates of PyC production (supplementary Figure S2).

The El Niño Southern Oscillation (ENSO) is the primary driver of inter-annual variability in burned area in the tropics[45] and previous analyses conducted with GFED have shown that carbon emissions from tropical forest ecosystems more than doubled on average during positive (El Niño) phases relative to negative (La Niña) ENSO phases[46]. Correspondingly, we calculated that global rates of PyC production in tropical forests were 111% greater during the main fire season of El Niño phases than La Niña phases (supplementary Table S1). As rates of PyC production by non-forest fires did not show a significant response to ENSO at the global scale (supplementary Table S1), the response of forest fires was the major driver of inter-annual variability in total PyC production (Figure 3). The production of PyC was anomalously high in 1997-1998 (366 Tg C year^{-1}), aligning with a particularly strong positive El Niño phase which promoted extensive burning of (tropical) forests in South and Central America and in Southeast and Equatorial Asia[1,46].

Submitted manuscript draft of version of: Jones, M.W., Santín, C., van der Werf, G.R., **Doerr, S.H.** (2019) Global fire emissions buffered by the production of recalcitrant pyrogenic carbon. *Nature Geoscience* (published on 5th Aug. 2019, available at: https://doi.org/10.1038/s41561-019-0403-x). Note that the published version will be an updated version from this submitted draft.

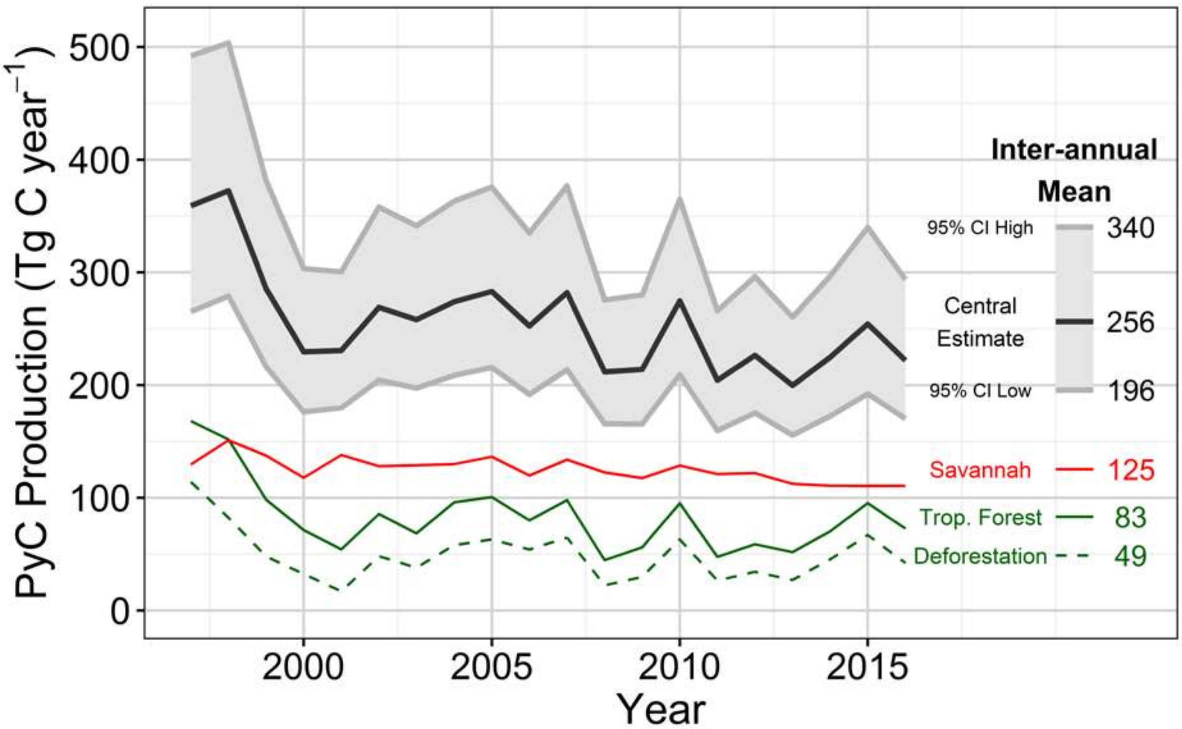

Figure 3: Annual global PyC production estimates from GFED4s+PyC. The black line plots the modelled rate of production based on central P_{PyC} ratios (g PyC g^{-1} C emitted) from the global dataset. The shaded area indicates the uncertainty range of modelled values based on the 95% confidence intervals of P_{PYC} values (see Figure 2). The contributions of savannah burning and tropical forest burning to global production totals are shown, the latter of which includes deforestation fires (also shown; dashed line).

Major Production Regions

The PyC production rates modelled by GFED4s+PyC conformed to a latitudinal pattern (Figure 4), with the tropical latitudes clearly dominating production at the global scale. 91% of global production occurred in the tropics and subtropics (0-30° N/S), while temperate (30-60° N/S) and high-latitude regions (60-90° N) provided small contributions to the global total (8% and 1%, respectively).

The global distribution of PyC production also showed intricate regional patterns driven by variation in both the frequency at which fuel stocks were exposed to fire and the magnitude of the fuel stocks that were combusted during the fires that occurred (supplementary Figures S3 and S4). Fire frequency was ultimately the key determinant of PyC production rate and this explains why the tropics and subtropics were the dominant source regions. Although savannah fires affected low fuel stocks (0.2 kg C km^{-2} on average; supplementary information text S2), these fires occurred frequently and were spatially extensive (supplementary Figure S5 and table S2). They thus made the largest contribution to the global PyC production flux (125 Tg C year^{-1} on average). Although tropical deforestation fires affected approximately 1% of the area of savannah fires, they affected large stocks of fuel (8.7 kg C km^{-2} on average; supplementary table S2) and were thus second largest driver of global PyC production, contributing 49 Tg C year^{-1}. The area affected by non-deforestation tropical forest fires was more than a factor of 4 larger than that of deforestation fires, however fuel consumption was relatively low (2.3 kg C km^{-2} on average; supplementary table S2). These fires provide the third major component of the global PyC production flux (34 Tg C year^{-1}). Overall, 81% of total global PyC production in the period 1997-2016 occurred in savannahs (49%) and tropical forests (32%).

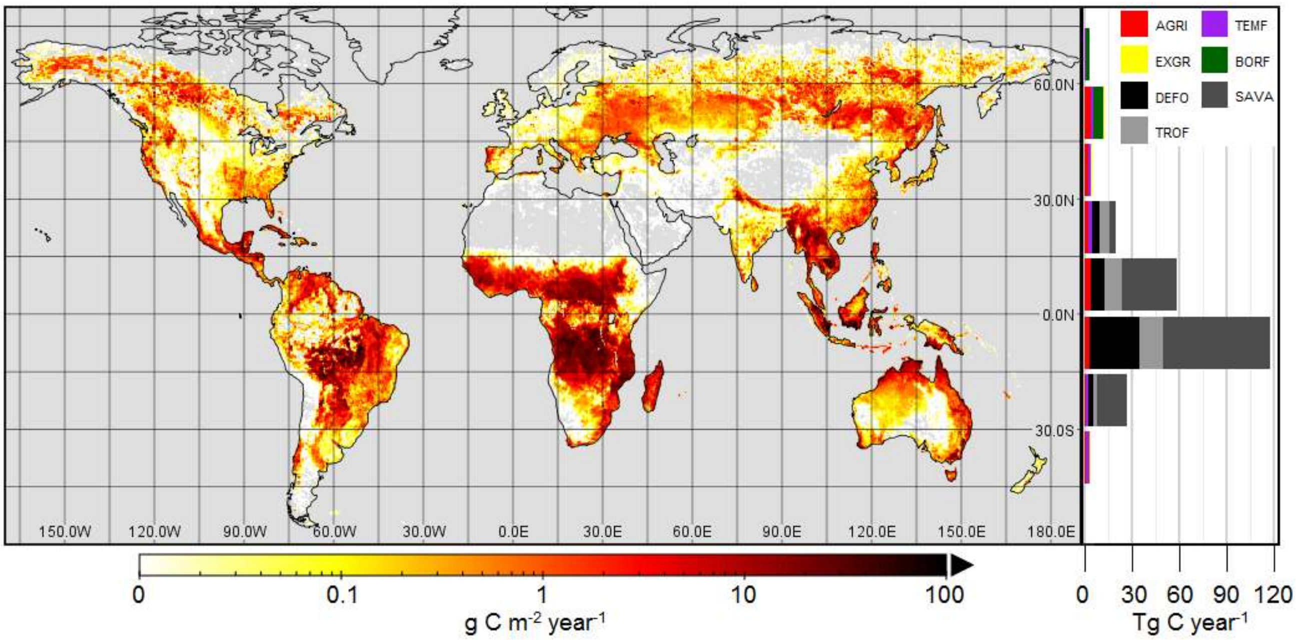

Figure 4: Annual average PyC production rates for the period 1997-2016 from GFED4s+PyC, based on central production factors (see Figure 2). **(Left panel)** The global distribution of PyC production expressed in g C m^{-2} year^{-1}. **(Right panel)** The total production of PyC (Tg C year^{-1}) in 15° latitudinal bands segregated according to the fire type, including: savannah fires (SAVA); non-deforestation tropical forest fires (TROF); tropical deforestation fires (DEFO); agricultural fires (AGRI); temperate forest fires (TEMF); extratropical grassland fires (EXGR), and; boreal forest fires (BORF).

Global Carbon Budget Implications

Here we have quantified the global gross sink of atmospheric carbon caused by the transfer of photosynthetically-sequestered biomass carbon to stocks of PyC during vegetation fires. Our central global PyC production flux estimate (256 Tg C year^{-1}) is nontrivial within the context of the global carbon cycle (Figure 1), equating to 12% of the global carbon emissions flux due to biomass burning and around 8% of the land sink for atmospheric CO_2 (~3.0-3.2 Tg C year^{-1})[2,4]. This flux is in addition to the smaller global flux of 2 Tg C year^{-1} caused by the emission of PyC in smoke from vegetation fires (according to estimates made using GFED4s in the years 1997-2016)[1].

The magnitude of our global estimate for PyC production indicates that the transformation of biomass carbon to PyC in vegetation fires has the potential to significantly influence the atmospheric stock of carbon. A net sink of atmospheric carbon to stocks of PyC can be expected to develop if the flux associated with its production is unmatched by re-mineralisation fluxes from legacy PyC stocks in terrestrial and marine pools (Figure 1). Earth System Models (ESMs) are the most sophisticated tools available to quantify the exchange of carbon between the atmosphere and these pools in time periods for which robust empirical data is sparse or unavailable. Despite foregoing attempts to highlight the importance of PyC production for carbon storage over timescales relevant to anthropogenic climate change and its mitigation[36,37,47], the absence of the PyC cycle from ESMs has restricted the scope for quantifying its role in the carbon cycle[15]. The method introduced here allows for the routine integration of PyC production into fire-enabled vegetation models in a manner that systematically considers the spatial distribution of fire, the composition of the fuel stocks affected and the specific PyC production factors that apply to individual fuel components. This procedure would be relatively simple to implement in other fire-enabled vegetation models used by ESMs, meaning that the major outstanding challenge to quantifying the net exchange of carbon between the atmosphere and PyC stocks with ESMs will be to improve constraints over its storage and residence time in terrestrial and marine pools (Figure 1)[14,15].

We also show that the PyC cycle must be integrated into ESMs if they are to accurately represent the more general role of fire in the carbon cycle. At present, the fate of 11% of the global biomass carbon stocks affected annually by fire is misrepresented in global models. Recent estimates suggest that total carbon emissions from biomass burning in the period

1750-2015 amounted to around 500 Pg C (averaging 1.9 Pg C year^{-1})[41]. Under the assumption that the modern global PyC production flux maintained a constant ratio with the carbon emissions flux throughout this period, we estimate that approximately 60 Pg C was transferred to PyC stocks since the beginning of the industrial revolution. This value is equivalent to 33-40% of the carbon lost from biomass pools due to land use change in the same time period (145-180 Pg C)[4,48].

The production flux of PyC represents the quantity of carbon that models would otherwise treat as unburned dead or living vegetation with a residence time in terrestrial pools on the order of months to decades[9,12,26,39,40,49]. This misrepresentation of the legacy effects of fire thus introduces potentially significant errors to carbon accounting exercises. Moreover, as PyC dynamics are not represented in the ESMs used to make global carbon budget calculations, this pool may represent a missing sink or source of carbon to the atmosphere[15,50]. Our PyC production estimate is equivalent to 41% of the global carbon budget imbalance caused by overestimated emissions and/or underestimated sinks in the past decade (600 Tg C year^{-1})[2], suggesting that errors resulting from the absence of PyC from ESMs may contribute significantly to global carbon accounting uncertainties.

The production of PyC may also become an increasingly important process for global carbon cycling in future centuries. Although global burned area has declined in at least the past two decades due predominantly to the conversion of savannah and grassland to agriculture[51,52], recent fire modelling studies generally agree that this decline is unlikely to continue past the year 2050[53–55]. It is also likely that a higher fraction of global burned area will be distributed in forests where significant stocks of vegetation carbon are held[54,56,57]. As woody fuels generate more PyC per unit of biomass carbon than other fuels (Figure 1), the spread of fire into forests can be expected to disproportionately enhance global PyC production (supplementary Figure S2). Although it is less clear how fire prevalence will change in tropical and temperate forests owing to a stronger human control over burning in these regions[51,54], recent increases in fire extent caused by increasing drought frequency in Amazonia are already counteracting reductions in the extent of deforestation fires[58]. Notwithstanding the significant uncertainty that exists in model predictions of future fire regimes, there are strong indications that PyC production rates will increase in some of the Earth's most carbon-dense regions in response to a changing climate[7,9,59]. This implies that the buffer for atmospheric CO_2 emissions resulting from PyC production will grow in future centuries.

Methods

Global Fuel Consumption Modelling in GFED4s

In GFED4s, carbon emissions to the atmosphere are quantified based on burned area and fuel consumption per unit burned area. Burned area is derived from satellite[60] and fires that are too small to be detected by regular burned area algorithms are derived statistically based on active fire detections and relations with vegetation indices[61]. Fuel consumption is modelled using a satellite-driven biogeochemical model[1] and tuned to match observations[62]. Most of the underlying satellite input datasets have a 500 × 500 m resolution but are aggregated to the model resolution of 0.25° × 0.25°. Total fuel consumption is based on fuel consumption of several fuel components including leaves, grasses, litter, fine woody debris, coarse woody debris (CWD), and standing wood. For more information on the GFED4s modelling approach, the reader is directed to reference[1].

To calculate PyC production within GFED4s we added a production factor, P_{PYC}, which quantifies the production of PyC per unit carbon emitted (g PyC g^{-1} C emitted). Until now, the principle obstacle to performing a global modelling exercise of this type has been the lack of a sufficiently rich and standardised dataset with which to constrain representative values for P_{PYC}. The remainder of this section details how representative PyC production factors were collated and summarised and subsequently integrated into the fuel consumption model of GFED4s.

Our estimates of uncertainty in PyC production relate only to variability in PyC production factors and do not include uncertainty in fuel consumption propagating from GFED4s. Uncertainties in GFED4s fuel consumption are discussed in great detail in ref. [1] and are predominantly the result of uncertainties in the satellite detection of small fires using thermal anomalies and burn scars. Based on the level of agreement with regional-level estimates it is estimated that the burned area data used in GFED have a 1 standard deviation uncertainty range of 50% but are probably underestimated due to the difficulty in capturing small fire burned area and the choice of a conservative approach in ref. [61]. As carbon emissions and PyC production are co-dependent on burned area, estimation errors relating to fire detection introduce scalar uncertainties. Uncertainty in fuel consumption is a smaller component of the overall uncertainty in GFED4s[1] emission estimates and has been reduced from previous versions through its incorporation of a global dataset of fuel consumption estimates[62].

Collating a Global Dataset of PyC Production Factors

We compiled a new database of P_{PYC} factors from a global collection of 21 published studies which reported on PyC production in 91 burn units, as well as two new datasets produced by the authors with 23 burn units reported for the first time here, and standardised their reporting. All studies used one of the following two broad approaches to quantifying the impacts of fire on the biomass carbon stocks, either: pre-fire and post-fire stocks of biomass carbon and PyC are measured, or; space-for-time substitution is used to constrain burned and unburned stocks of biomass carbon and PyC, which are assumed to be equivalent to pre-fire and post-fire stocks, respectively. Hereafter, the terms “pre-fire” and “post-fire” are used to refer to both types of assessment. Here we focus only on PyC present in charcoal and ash on the ground following fire[63] as well as charred vegetation. PyC emitted with smoke, transported in the atmosphere and deposited over a distant area is not included as this process has been studied in separate dedicated studies conducted by atmospheric scientists[24] and represents a relatively small flux in comparison (<5%)[13,14].

The P_{PYC} values were calculated for each of six classes of widely used biomass components: coarse woody surface fuels (CWSF), including coarse woody debris or downed wood defined by typical diameter thresholds of >7.6 cm or >10 cm[64,65]; fine woody surface fuels (FWSF), including fine woody debris or any other woody debris with diameters below the thresholds for CWSF; coarse woody aboveground fuels (CWAGF), including trees or branches with diameters greater than the thresholds for CWSF; fine woody aboveground fuels (FWAGF), including material described as shrubs, trees or branches with diameters below the thresholds for CWSF; non-woody surface fuels (NWSF), including litter, understory vegetation, grass, root mat and any other form of non-woody material directly in contact with the ground surface[65,66], and finally; non-woody aboveground fuels (NWAGF), including foliage, leaves, needles, crown fuels and any other form of non-woody material that attaches to standing wood structures above the ground surface.

For each biomass component, P_{PYC} was calculated using the following equation (1):

Submitted manuscript draft of version of: Jones, M.W., Santín, C., van der Werf, G.R., **Doerr, S.H.** (2019) Global fire emissions buffered by the production of recalcitrant pyrogenic carbon. *Nature Geoscience* (published on 5th Aug. 2019, available at: https://doi.org/10.1038/s41561-019-0403-x). Note that the published version will be an updated version from this submitted draft.

$$P_{PyC} = \frac{C_{Py}}{C_{PRE} - C_{POST}}$$

where C_{Py} is the mass of PyC created during the fire that was attributed to the component, C_{PRE} was the pre-fire stock of biomass carbon in the component, and C_{POST} was the post-fire stock of biomass carbon in the component. C_{Py}, C_{PRE} and C_{POST} were all expressed in the units g C km^{-2}.

Criteria were applied as filters to the dataset in order to ensure that P_{PYC} could be calculated in a consistent and representative manner. Specifically, P_{PYC} was calculated if the following conditions were met: first, both pre-fire and post-fire biomass stocks were reported and carbon content (%) was either measured or assumed based on representative values from the literature; second, post-fire stocks of pyrogenic organic matter (charcoal, ash and charred vegetation) were reported and their PyC content (%) was either measured or assumed based on representative values from the literature; third, the type of fire that occurred was representative of a widespread regional fire type (e.g. wildfires, slash-and-burn deforestation, and prescribed fire); fourth, in experimental fires, the biomass carbon stock was designed to replicate the density and structure of biomass carbon stocks observed in the field and the burning efficiency was not optimised or adapted as a factor of the study design; fifth, the post-fire sampling exercise was completed within 3 months of the fire such that losses of PyC through erosion and mineralisation were minimised.

Like biomass carbon, total PyC stocks are distributed across several components including charcoal and ash on the ground, charcoal attached to coarse woody debris, and charcoal attached to aboveground vegetation[13]. The majority of the studies included in the production factor dataset matched the studied PyC components to individual biomass carbon components from which they were known to derive. However, as some individual components of PyC stocks can have a mixture of sources that are indistinguishable from their location or appearance alone, it was occasionally necessary to make assumptions about the biomass components that were sources of these components. This was done on a study-by-study basis. In cases where the source of each PyC component was not explicitly stated, the following procedural steps were adhered to. On a first basis, the PyC component was assigned to a biomass component according to the most probable source inferred, but not explicitly stated, in the primary literature. Second, where more than one biomass component was inferred to be a source of the PyC stock in the primary literature, the PyC stock was weighted proportionally to the pre-fire stock of carbon present in each of the implicated biomass components. Otherwise, if no sources of PyC were inferred in the primary literature it was necessary to make independent assumptions about the source of PyC in a manner that was consistent with the other studies included in the dataset and our collective experience of quantifying PyC production in the field.

Summarising Production Factor Values for use in GFED4s+PyC

Our global database suggested that coarse woody surface fuels (CWSF) and aboveground fuels (CWAGF) produce significantly more PyC, relative to carbon emitted, than other fuel classes (P_{PYC} averaged 0.25 and 0.31 g PyC g^{-1} C emitted, respectively; Figure 2). In contrast, the mean P_{PYC} values for fine woody surface fuels (FWSF) and fine woody aboveground fuels (FWAGF; 0.12 and 0.076 g PyC g^{-1} C emitted, respectively) did not differ significantly from those of non-woody surface fuels (NWSF) or non-woody aboveground fuels (NWAGF; 0.099 and 0.062 g PyC g^{-1} C emitted, respectively). These results are consistent with previous studies, which suggest that large-diameter woody fuels burn less completely and produce PyC in greater proportions than finer fuels[23,36,67].

For each class, the mean PyC production factor was used as the central estimate for P_{PYC}, while the confidence interval around the mean P_{PYC} was calculated through a bootstrapping procedure. Specifically, the available PyC production factors from the dataset were resampled 50,000 times, the mean P_{PYC} was calculated for each resample, and the 95% confidence interval was calculated as the middle 95% of the observed 50,000 means (i.e. those ranked 1,250th to 48,750th).

According to analysis of variance (ANOVA) with a Tukey Honest Significant Difference post-hoc test, no significant differences in mean P_{PYC} were observed between the distributions of P_{PyC} for coarse, fine, and non- woody fuels positioned at the ground surface and those same fuels located above the ground surface. Therefore, the P_{PYC} values applied in GFED4s+PyC were based on the distribution of values in three simplified fuel classes (Figure 2): coarse woody fuels (CWF: mean 0.26 g PyC g^{-1} C; 95% confidence interval 0.18-0.39 g PyC g^{-1} C), fine woody fuels (FWF: mean 0.096 g PyC g^{-1} C; 95% confidence interval 0.064-0.15 g PyC g^{-1} C) and non-woody fuels (NWF: mean 0.091 g PyC g^{-1} C; 95% confidence interval 0.074-0.11 g PyC g^{-1} C).

Assigning PyC Production Factors in GFED4s+PyC

P_{PyC} values were assigned to each of the native fuel classes of GFED4s[1], which are: leaves; grasses; surface fuels (including litter and fine woody debris); coarse woody debris (CWD), and; standing wood (including trunks, stems and branches). Mean P_{PyC} values and bootstrapped confidence interval values for CWF, FWF and NWF from the global dataset were used to define representative P_{PyC} values for each of the GFED4s fuel classes (Figure 2). Full details regarding the assignment of P_{PyC} values to each GFED4s fuel class are provided in the supplementary information (text S3 and table S3). Briefly: leaf, litter, grass were assigned the relevant P_{PyC} values of NWF; fine woody debris and coarse woody debris were assigned the values of FWF and CWF, respectively, and; P_{PyC} values for standing wood were applied in a spatially explicit manner as weighted combinations of the P_{PyC} values for CWF (for carbon in trunks) and FWF (for carbon in branches). The weighted CWF:FWF ratio was assigned according to empirical relationships defining biomass carbon apportionment to branches and trunks in the various forest types of the GFED4s land cover scheme (supplementary information text S3 and table S4)[68].

Quantifying ENSO Impacts on PyC Production

To investigate the influence of pan-tropical climatic variability driven by the El Niño Southern Oscillation on the production of PyC, we replicated the analysis presented by Chen et al. (ref. [46]) with a focus on PyC production rather than carbon emissions. The pan-tropics were defined as consisting of Central America (CEAM); Northern Hemisphere South America (NHSA); Southern Hemisphere South America (SHSA); Northern Hemisphere Africa (NHAF); Southern Hemisphere Africa (SHAF); Southeast Asia (SEAS); Equatorial Asia (EQAS), and; Australia (AUST; supplementary Figure S6). PyC production in El Niño and La Niña phases was compared for the major fire season periods defined in each tropical region by Chen et al. (ref. [46]); the reader is referred to their study for a thorough explanation of the rationale for selecting these comparison periods. We summed PyC production in the major fire season period of each region and disaggregated this total to forest and non-forest fires according to the dominant land cover type in the GFED4s land cover scheme (based on the MODIS Land Cover Type Climate Modelling Grid product MCD12C1)[69].

Apportioning Sources of PyC

Following GFED4s+PyC model runs, PyC production was assigned to specific sources following a method developed previously for use in GFED4s model runs[1,70]. Specifically, PyC production occurring as a result of non-deforestation fires was disaggregated in each cell to tropical forest, savannah/grassland, boreal forest, temperate forest, and agricultural fires using an existing algorithm that utilises fractional tree cover, climate and fire persistence variables. The reader is referred to ref. [70] for a full discussion of this algorithm. We added an additional latitudinal constraint (30 °N-30 °S) to further disaggregate the savannah compartment, which thus separates tropical savannahs and grasslands from extratropical grasslands.

References

1. van der Werf, G. R. *et al.* Global fire emissions estimates during 1997–2016. *Earth Syst. Sci. Data* **9,** 697–720 (2017).
2. Le Quéré, C. *et al.* Global Carbon Budget 2018. *Earth Syst. Sci. Data* **10,** 2141–2194 (2018).
3. Houghton, R. A. & Nassikas, A. A. Global and regional fluxes of carbon from land use and land cover change 1850-2015. *Global Biogeochem. Cycles* **31,** 456–472 (2017).
4. Ciais, P. *et al.* in *Climate Change 2013: The Physical Science Basis. Contribution of Working Group I to the Fifth Assessment Report of the Intergovernmental Panel on Climate Change* (eds. Stocker, T. F. et al.) 465–570 (Cambridge University Press, 2013).
5. Crutzen, P. J. & Andreae, M. O. Biomass Burning in the Tropics: Impact on Atmospheric Chemistry and Biogeochemical Cycles. *Science* **250,** 1669–1678 (1990).
6. Ballantyne, A. P., Alden, C. B., Miller, J. B., Tans, P. P. & White, J. W. C. Increase in observed net carbon dioxide uptake by land and oceans during the past 50 years. *Nature* **488,** 70–72 (2012).
7. Bowman, D. *et al.* Fire in the Earth system. *Science* **324,** 481–4 (2009).
8. Pan, Y. *et al.* A Large and Persistent Carbon Sink in the World's Forests. *Science* **333,** 988–993 (2011).
9. Hantson, S. *et al.* The status and challenge of global fire modelling. *Biogeosciences* **13,** 3359–3375 (2016).
10. Rabin, S. S. *et al.* The Fire Modeling Intercomparison Project (FireMIP), phase 1: Experimental and analytical protocols with detailed model descriptions. *Geosci. Model Dev.* **10,** 1175–1197 (2017).
11. Kuhlbusch, T. A. J. Black Carbon and the Carbon Cycle. *Science* **280,** 1903–1904 (1998).
12. Lehmann, J. *et al.* Australian climate–carbon cycle feedback reduced by soil black carbon. *Nat. Geosci.* **1,** 832–835 (2008).
13. Santín, C. *et al.* Towards a global assessment of pyrogenic carbon from vegetation fires. *Glob. Chang. Biol.* **22,** 76–91 (2016).

14. Bird, M. I., Wynn, J. G., Saiz, G., Wurster, C. M. & McBeath, A. The Pyrogenic Carbon Cycle. *Annu. Rev. Earth Planet. Sci.* **43,** 273–298 (2015).
15. Landry, J.-S. & Matthews, H. D. The global pyrogenic carbon cycle and its impact on the level of atmospheric CO 2 over past and future centuries. *Glob. Chang. Biol.* **23,** 3205–3218 (2017).
16. Schmidt, M. W. I. Carbon budget in the black. *Nature* **427,** 305–307 (2004).
17. Reisser, M., Purves, R. S., Schmidt, M. W. I. & Abiven, S. Pyrogenic Carbon in Soils: A Literature-Based Inventory and a Global Estimation of Its Content in Soil Organic Carbon and Stocks. *Front. Earth Sci.* **4,** 1–14 (2016).
18. Ohlson, M., Dahlberg, B., Økland, T., Brown, K. J. & Halvorsen, R. The charcoal carbon pool in boreal forest soils. *Nat. Geosci.* **2,** 692–695 (2009).
19. Koele, N. *et al.* Amazon Basin forest pyrogenic carbon stocks: First estimate of deep storage. *Geoderma* **306,** 237–243 (2017).
20. Masiello, C. A. & Druffel, E. R. M. Black Carbon in Deep-Sea Sediments. *Science* **280,** 1911–1913 (1998).
21. Schmidt, M. W. I. & Noack, A. G. Black carbon in soils and sediments: Analysis, distribution, implications, and current challenges. *Global Biogeochem. Cycles* **14,** 777–793 (2000).
22. Dittmar, T. & Paeng, J. A heat-induced molecular signature in marine dissolved organic matter. *Nat. Geosci.* **2,** 175–179 (2009).
23. Wagner, S., Jaffé, R. & Stubbins, A. Dissolved black carbon in aquatic ecosystems. *Limnol. Oceanogr. Lett.* **3,** 168–185 (2018).
24. Bond, T. C. *et al.* Bounding the role of black carbon in the climate system: A scientific assessment. *J. Geophys. Res. Atmos.* **118,** 5380–5552 (2013).
25. Booth, B. & Bellouin, N. Black carbon and atmospheric feedbacks. *Nature* **519,** 167–168 (2015).
26. Kuzyakov, Y., Bogomolova, I. & Glaser, B. Biochar stability in soil: Decomposition during eight years and transformation as assessed by compound-specific14C analysis. *Soil Biol. Biochem.* **70,** 229–236 (2014).
27. Schneider, M. P. W., Hilf, M., Vogt, U. F. & Schmidt, M. W. I. The benzene polycarboxylic acid (BPCA) pattern of wood pyrolyzed between 200°C and 1000°C. *Org. Geochem.* **41,** 1082–1088 (2010).
28. Wiedemeier, D. B. *et al.* Aromaticity and degree of aromatic condensation of char. *Org. Geochem.* **78,** 135–143 (2015).
29. Jaffé, R. *et al.* Global charcoal mobilization from soils via dissolution and riverine transport to the oceans. *Science* **340,** 345–7 (2013).
30. Coppola, A. I. *et al.* Global-scale evidence for the refractory nature of riverine black carbon. *Nat. Geosci.* **11,** 584–588 (2018).
31. Coppola, A. I., Ziolkowski, L. A., Masiello, C. A. & Druffel, E. R. M. Aged black carbon in marine sediments and sinking particles. *Geophys. Res. Lett.* **41,** 2427–2433 (2014).
32. Singh, B. P., Cowie, A. L. & Smernik, R. J. Biochar Carbon Stability in a Clayey Soil As a Function of Feedstock and Pyrolysis Temperature. *Environ. Sci. Technol.* **46,** 11770–11778 (2012).
33. Ziolkowski, L. A. & Druffel, E. R. M. Aged black carbon identified in marine dissolved organic carbon. *Geophys. Res. Lett.* **37,** 4–7 (2010).
34. Preston, C. M. & Schmidt, M. W. I. Black (pyrogenic) carbon: a synthesis of current knowledge and uncertainties with special consideration of boreal regions. *Biogeosciences* **3,** 397–420 (2006).

Submitted manuscript draft of version of: Jones, M.W., Santín, C., van der Werf, G.R., **Doerr, S.H.** (2019) Global fire emissions buffered by the production of recalcitrant pyrogenic carbon. *Nature Geoscience* (published on 5th Aug. 2019, available at: https://doi.org/10.1038/s41561-019-0403-x). Note that the published version will be an updated version from this submitted draft.

35. Goldberg, E. D. *Black carbon in the environment: properties and distribution*. (John Wiley and Sons, 1985).
36. Kuhlbusch, T. a. J. & Crutzen, P. J. Toward a global estimate of black carbon in residues of vegetation fires representing a sink of atmospheric CO 2 and a source of O 2. *Global Biogeochem. Cycles* **9,** 491–501 (1995).
37. Santín, C., Doerr, S. H., Preston, C. M. & González-Rodríguez, G. Pyrogenic organic matter production from wildfires: a missing sink in the global carbon cycle. *Glob. Chang. Biol.* **21,** 1621–1633 (2015).
38. Singh, N., Abiven, S., Torn, M. S. & Schmidt, M. W. I. Fire-derived organic carbon in soil turns over on a centennial scale. *Biogeosciences* **9,** 2847–2857 (2012).
39. Schmidt, M. W. I. *et al.* Persistence of soil organic matter as an ecosystem property. *Nature* **478,** 49–56 (2011).
40. Thurner, M. *et al.* Evaluation of climate-related carbon turnover processes in global vegetation models for boreal and temperate forests. *Glob. Chang. Biol.* **23,** 3076–3091 (2017).
41. Van Marle, M. J. E. *et al.* Historic global biomass burning emissions for CMIP6 (BB4CMIP) based on merging satellite observations with proxies and fire models (1750-2015). *Geosci. Model Dev.* **10,** 3329–3357 (2017).
42. Yang, J. *et al.* Century-scale patterns and trends of global pyrogenic carbon emissions and fire influences on terrestrial carbon balance. *Global Biogeochem. Cycles* **29,** 1549–1566 (2015).
43. Schultz, M. G. *et al.* Global wildland fire emissions from 1960 to 2000. *Global Biogeochem. Cycles* **22,** 1–17 (2008).
44. Yang, J. *et al.* Spatial and temporal patterns of global burned area in response to anthropogenic and environmental factors: Reconstructing global fire history for the 20th and early 21st centuries. *J. Geophys. Res. Biogeosciences* **119,** 249–263 (2014).
45. Chen, Y., Morton, D. C., Andela, N., Giglio, L. & Randerson, J. T. How much global burned area can be forecast on seasonal time scales using sea surface temperatures? *Environ. Res. Lett.* **11,** (2016).
46. Chen, Y. *et al.* A pan-tropical cascade of fire driven by El Niño/Southern Oscillation. *Nat. Clim. Chang.* **7,** 906–911 (2017).
47. Woolf, D., Amonette, J. E., Street-Perrott, F. A., Lehmann, J. & Joseph, S. Sustainable biochar to mitigate global climate change. *Nat. Commun.* **1,** 1–9 (2010).
48. Houghton, R. A. & Nassikas, A. A. Global and regional fluxes of carbon from land use and land cover change 1850–2015. *Global Biogeochem. Cycles* **31,** 456–472 (2017).
49. Surawski, N. C., Sullivan, A. L., Roxburgh, S. H., Meyer, C. P. M. & Polglase, P. J. Incorrect interpretation of carbon mass balance biases global vegetation fire emission estimates. *Nat. Commun.* **7,** 1–5 (2016).
50. Santín, C., Doerr, S. H., Preston, C. M. & González-Rodríguez, G. Pyrogenic organic matter produced during wildfires can act as a carbon sink – a reply to Billings & Schlesinger (2015). *Glob. Chang. Biol.* **24,** e399 (2018).
51. Andela, N. *et al.* A human-driven decline in global burned area. *Science* **356,** 1356–1362 (2017).
52. Arora, V. K. & Melton, J. R. Reduction in global area burned and wildfire emissions since 1930s enhances carbon uptake by land. *Nat. Commun.* (2018). doi:10.1038/s41467-018-03838-0
53. Pechony, O. & Shindell, D. T. Driving forces of global wildfires over the past millennium and the forthcoming century. *Proc. Natl. Acad. Sci.* **107,** 19167–19170 (2010).

54. Knorr, W., Arneth, A. & Jiang, L. Demographic controls of future global fire risk. *Nat. Clim. Chang.* **6,** 781–785 (2016).
55. Flannigan, M. *et al.* Global wildland fire season severity in the 21st century. *For. Ecol. Manage.* **294,** 54–61 (2013).
56. Flannigan, M. D. *et al.* Fuel moisture sensitivity to temperature and precipitation: climate change implications. *Clim. Change* **134,** 59–71 (2016).
57. Wang, X. *et al.* Projected changes in daily fire spread across Canada over the next century. *Environ. Res. Lett.* **12,** (2017).
58. Aragão, L. E. O. C. *et al.* 21st Century drought-related fires counteract the decline of Amazon deforestation carbon emissions. *Nat. Commun.* **9,** 536 (2018).
59. Krawchuk, M. A. & Moritz, M. A. Burning issues: statistical analyses of global fire data to inform assessments of environmental change. *Environmetrics* **25,** 472–481 (2014).
60. Giglio, L., Randerson, J. T. & van der Werf, G. R. Analysis of daily, monthly, and annual burned area using the fourth-generation global fire emissions database (GFED4). *J. Geophys. Res. Biogeosciences* **118,** 317–328 (2013).
61. Randerson, J. T., Chen, Y., Van Der Werf, G. R., Rogers, B. M. & Morton, D. C. Global burned area and biomass burning emissions from small fires. *J. Geophys. Res. Biogeosciences* **117,** (2012).
62. van Leeuwen, T. T. *et al.* Biomass burning fuel consumption rates: a field measurement database. *Biogeosciences Discuss.* **11,** 8115–8180 (2014).
63. Bodí, M. B. *et al.* Wildland fire ash: Production, composition and eco-hydro-geomorphic effects. *Earth-Science Rev.* **130,** 103–127 (2014).
64. Hyde, J. C., Smith, A. M. S., Ottmar, R. D., Alvarado, E. C. & Morgan, P. The combustion of sound and rotten coarse woody debris: a review. *Int. J. Wildl. Fire* **20,** 163 (2011).
65. Lutes, D. C., Keane, R. E. & Caratti, J. F. A surface fuel classification for estimating fire effects. *Int. J. Wildl. Fire* **18,** 802 (2009).
66. Sandberg, D. V., Ottmar, R. D. & Cushon, G. H. Characterizing fuels in the 21st Century. *Int. J. Wildl. Fire* **10,** 381 (2001).
67. Knicker, H., Hilscher, A., González-Vila, F. J. & Almendros, G. A new conceptual model for the structural properties of char produced during vegetation fires. *Org. Geochem.* **39,** 935–939 (2008).
68. Thurner, M. *et al.* Carbon stock and density of northern boreal and temperate forests. *Glob. Ecol. Biogeogr.* **23,** 297–310 (2014).
69. Friedl, M., Sulla-Menashe, D. MCD12C1 MODIS/Terra+Aqua Land Cover Type Yearly L3 Global 0.05Deg CMG V006. (2015). doi:10.5067/MODIS/MCD12C1.006
70. van der Werf, G. R. *et al.* Global fire emissions and the contribution of deforestation, savanna, forest, agricultural, and peat fires (1997–2009). *Atmos. Chem. Phys.* **10,** 11707–11735 (2010).
71. van der Werf, G. R. *et al.* Interannual variability in global biomass burning emissions from 1997 to 2004. *Atmos. Chem. Phys.* 3423–3441 (2006).

Supplementary Information is linked to the online version of the paper at www.nature.com/nature.

Acknowledgements

This work was funded by the Leverhulme Trust Grant awarded to SD (RPG-2014-095); a Swansea University College of Science Fund awarded to MJ; a Vici grant awarded to GW by the Netherlands organisation for scientific research (NWO), and a European Union Horizon 2020 research and innovation grant awarded to CS (Marie Skłodowska-Curie grant 663830). We thank Cristina Aponte, Claudia Boot, Gareth Clay, Garry Cook, Francesca Cotrufo, Philip Fearnside, Brett Goforth, Robert Graham, Michelle Haddix, Peter Homann, Dale Hurst and Meaghan Jenkins for their assistance during the collation of the global dataset of PyC production factors. We also thank Dr. Bill de Groot for his part in securing funding of the Leverhulme Trust Grant.

Author Contributions

MJ, CS and SD designed the study. SD led the Leverhulme Trust grant funding the majority of the work. MJ collated the PyC production factor dataset with support from CS. CS and SD provided unpublished PyC production data. GW provided access to the GFED4s code. MJ adapted the GFED4s code to include PyC production with the support of GW. MJ conducted the formal analysis of production factor dataset and model outputs. All authors contributed to the interpretation of the results. MJ wrote the manuscript text and produced all figures. All authors contributed to the refinement of the manuscript text.

Author Information

Reprints and permissions information is available at www.nature.com/reprints. The authors declare no competing interests. Correspondence and requests for materials should be addressed to matthew.w.jones@swansea.ac.uk. The global dataset of PyC production factors is available as supplementary data file (GlobalPyC_supplementarydataset.xls) and will also be made publicly available through submission to the Pangaea Data Publisher for Earth & Environmental Science. Supplementary informaion text S4 contains full reference to the studies included in the production factor dataset.